A bacteriophage-based hyperpolarized ^{129}Xe MRI contrast agent targeting the EGF receptor in mammalian cells

Richard Matthew Ramirez[1,2], Krishnan K Palaniappan[1], David E Wemmer[1,3], Matthew B Francis[1,2], and Alex Pines[1,2]

[1]*Department of Chemistry, University of California, Berkeley, CA, United States,* [2]*Materials Science Division, Lawrence Berkeley National Laboratory, Berkeley, CA, United States,* [3]*Physical Biosciences Division, Lawrence Berkeley National Laboratory, Berkeley, CA, United States*

Introduction

Conventional NMR techniques do not discriminate well between healthy and diseased tissues, which is important for diagnostic imaging purposes. Furthermore, they lack the sensitivity necessary to detect small quantities of biomarkers required for early detection of diseased states (e.g. cancer). Xenon-129 is an attractive option because large signals can be generated from small quantities of Xe through hyperpolarization (1), and it can be localized via cryptophane-based biosensors (2-7). Exchange of Xe between cryptophane-A (CryA) and bulk solution can be exploited for chemical exchange saturation transfer (CEST) (3), which affords better sensitivity that direct detection methods. Protein scaffolds such as viral capsids and bacteriophages have been utilized for the multivalent display of many CryA moleculcules per agent, increasing contrast efficiency (8, 9). Additionally, phage-display techniques provide immediate access to a variety of bacteriophages against biologically relevant targets as there are many techniques for introducing targeting moieties such as antibodies, peptides, DNA. *The objective of this study is to demonstrate live-cell imaging using a bacteriophage-based xenon biosensor that selectively binds an EGFR-positive cell-line and is detected by hyperCEST.*

Methods

A targeted Xe biosensor was created from the protein scaffold of Fd filamentous bacteriophage (Fig. 1) which display scFv antibody fragments against the epidermal growth factor receptor (EGFR) on each of their p3 minor coat proteins (10). Phage were site-specifically modified to introduce the Xe-binding molecular cage, CryA, to the N-terminus of their major coat protein (~4200 copies) following previously optimized conditions (9). Typical modification was 9%, resulting in an anti-EGFR Fd phage-CryA biosensor (Fd-biosensor) with ~380 CryA molecules. For cell labeling experiments, 180 million cells of either a human breast cancer cell-line overexpressing EGFR, MDA-MB-231, or control cell-line derived from a human T-cell leukemia, Jurkat, were incubated 2 h at 4 °C with a 3 mL solution of 0.7 nM Fd-biosensor in phosphate buffered saline with 1% bovine serum albumin (PBS). Cells were washed three times with PBS to remove any transiently bound Fd-biosensor, and half of these labeled cells were prepared for NMR analysis by suspending in 500 uL of PBS. A non-ionic surfactant, Pluronic L-81, was added to final concentration of 0.01% (v/v) to decrease surface tension and control foaming. NMR experiments were conducted on a 300 MHz Varian ^{UNITY}INOVA spectrometer using a dual-tuned (^{1}H, ^{129}Xe) 5mm probe. A xenon gas mixture (2%:10%:88% Xe natural abundance/N_2/He) was hyperpolarized by spin exchange optical pumping using a commercial polarizer (MITI XenoSpin, formerly Nycomed Amersham, now GE). The hyperpolarized Xe gas mixture was delivered via plastic tubing to a 5mm NMR tube modified to include gas inlet and outlet arms. Samples were bubbled for 10 s at 0.4 SLM, followed by a 10 s wait period to allow bubbles to clear and foaming to subside. Temperature was regulated at 37 °C for all experiments. Z-spectra were collected for MDA, Jurkat, and PBS solutions using a 4 s, 21 μT continuous wave (cw) saturation pulse applied at 79 evenly-spaced offsets between 29 and 264 ppm (referenced to Xe gas). Saturation curves were obtained by varying the saturation duration of a cw saturation pulse applied at either the known CryA chemical shift ("on-resonance"), or at an equal distance downfield from the chemical shift of Xe dissolved in water ("off-resonance"). All signals were acquired in a single shot with a 25 kHz spectral width and 500 ms acquisition time following excitation with a hard pulse. Data processing and analysis were performed in MATLAB (R2010a v 7.10, The MathWorks). Cell viability was assessed before and after Xe experiments by staining cells with Trypan blue and counting using a hemocytometer.

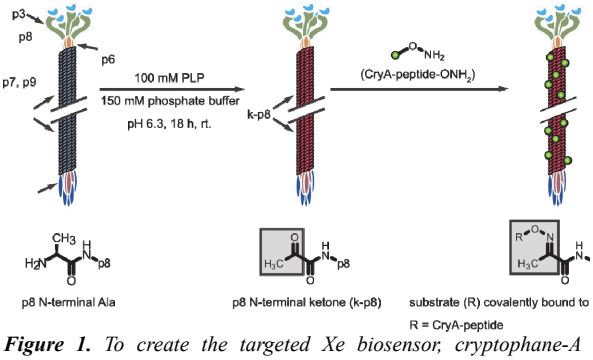

Figure 1. *To create the targeted Xe biosensor, cryptophane-A molecular cages were covalently attached to the p8 major coat protein of an Fd bacteriophage displaying scFv antibody fragments against the EGF receptor.*

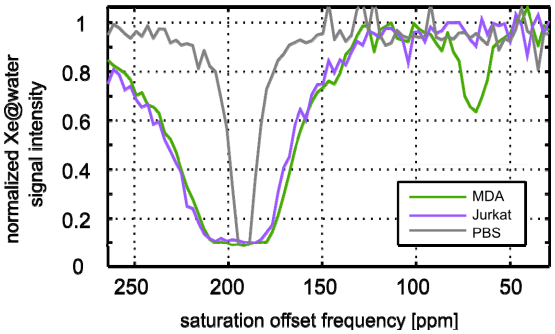

Figure 2. *Z-spectra were obtained for MDA, Jurkat, and PBS solutions using a 21 μT, 4 s cw saturation pulse. The dip observed at ~68 ppm in the MDA solution corresponds to the Fd-biosensor, which is not present in the Jurkat solution.*

Results

Comparison of z-spectra (Fig. 2) clearly showed that the Fd-biosensor was present in the MDA cell solution and not in the Jurkat cell solution, as evidenced by the dip in Xe@water signal intensity at 68 ppm. Both cell solutions showed a broad, asymmetric response to saturation pulses centered near the Xe@water chemical shift of 192 ppm, whereas the PBS-only solution had a much narrower, symmetric response (Fig. 2). Saturation curves at the same intensity and higher (data not shown) further indicated the presence of the Fd-biosensor construct in MDA solutions, but not in Jurkat solutions. Analysis of cell viability via Trypan blue staining showed that a majority of cell membranes remained uncompromised after 2 hours of Xe bubbling (Fig. 3).

Discussion

The results demonstrate successful discrimination of cell phenotype by the Fd-biosensor. CEST contrast was not observed in Jurkat cell solutions, meaning that none or very little of the agent was taken up or otherwise bound through non-specific interactions or other mechanisms not mediated by the EGF receptor. This study did not address whether the Fd-biosensor was internalized or remained peripherally bound to the cell. It is unknown whether endocytosis will affect the hyperCEST method. Recent reports show unique chemical shifts for Xe in cells (7, 11) , and although a second peak was not observed in the ^{129}Xe NMR spectrum, it is hypothesized that the broad, asymmetric saturation response centered around 192 ppm in the z-spectra is due to the presence of a second Xe pool downfield, namely Xe inside/associated with cells. This suggests that Xe transport across these cell membranes is fast. Given that the response of both Jurkat and MDA cell solutions was the same, it would also rule out slow Xe transport as a potential reason why no CEST contrast was observed in Jurkat cells. The amount of Fd-biosensor agent retained by the MDA cells is the subject of further investigation, as is the minimum number of cells needed for detection. These questions will depend on a several variables such as incubation conditions (e.g. time and temperature), and saturation parameters. The utility of frequency-selective dSNOB saturation schemes has been highlighted recently (12) and used to achieve low detection thresholds with similar CryA-based protein-scaffold constructs *in vitro* (8, 9). Additionally, experimental parameters will be optimized to decrease cell death, in particular for MDA cell solutions. This could include using growth media for NMR experiments rather than PBS, as well as lowering the flow rate and/or bubbling time to minimize stress on the cells.

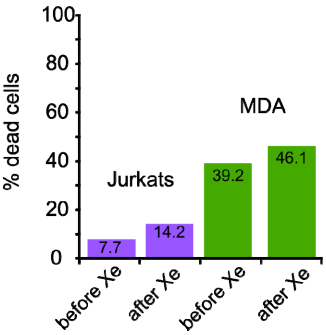

Figure 3. *Aliquots of cell solutions were saved before and after Xe NMR experiments to assess cell membrane integrity via Trypan blue staining.*

References

(1) Goodson BM. *J. Magn. Reson*. **2002**, 155, 157-216. (2) Spence MM et al. *J. Am. Chem. Soc*. **2004**. (3) Schroder L et al. *Science*. **2006**, 314, 446. (4) Wei Q et al. *J. Am. Chem. Soc*. **2006**, 1235-1239. (5) Roy V et al. *ChemPhysChem*. **2007**, 8, 2082-5. (6) Chambers JM et al. *J. Am. Chem. Soc*. **2009**, 131, 563-569. (7) Boutin C et al. *Bioorg. & Med. Chem*. **2011**, 19, 4135-43. (8) Meldrum TK et al. *J. Am. Chem. Soc*. **2010**, 132, 5936–5937. (9) Stevens TK et al. *Proc. of the ISMRM* **2010**. (10) Zhou Y et al. *J. Mol. Biol*. **2007**, 371, 934-47. (11) Boutin C et al. *NMR in Biomed*. **2011**, 24. (12) Meldrum TK et al. *J. Magn. Reson*. **2011**, 213, 14-21.